# Levee body seepage: a refinement of an expeditious procedure for fragility curves and vulnerability diagrams' assessment

Silvia Barbetta, Stefania Camici, Paola Bertuccioli, Michela Rosa Palladino and Tommaso Moramarco

## ABSTRACT

Extensive flooding can be the result of levee system failures most frequently caused by the piping process due to seepage. The proper description of the seepage line is affected by the difficulty of estimating the hydraulic parameters, mainly the soil hydraulic conductivity. Therefore, the development of simple methods for a quick analysis of extended levee systems is fundamental to identify critical points. In this context, a practical procedure, recently proposed, based on a simple vulnerability index is here enhanced and used to derive diagrams easily applicable for seepage vulnerability estimate, taking the hydraulic parameters' uncertainty into account. The procedure is applied for the Tiber River, in central Italy, and the Tanaro River, in northern Italy, by analyzing 67 and 6 levees, respectively. The results show that the method provides the highest seepage probabilities for levees affected by failures in the past. Therefore, the procedure seems to be able to identify the levees that require detailed investigations. Finally, the Italian levee database (DANTE) is presented as a dynamic geospatial tool for collecting all the available data/information on levee systems to usefully support authorities with the charge of hydraulic risk mitigation for identifying the most vulnerable levees.

**Key words** | levee database, levee failure, piping, seepage, seepage vulnerability diagrams, vulnerability index

**Silvia Barbetta** (corresponding author)
**Stefania Camici**
**Tommaso Moramarco**
National Research Council, IRPI,
Via Madonna Alta 126,
06128 Perugia,
Italy
E-mail: *s.barbetta@cnr.irpi.it*

**Paola Bertuccioli**
Italian Civil Protection Department,
Via Vitorchiano 2,
00189 Roma,
Italy

**Michela Rosa Palladino**
Politecnico di Torino,
Corso Duca degli Abruzzi, 24,
Torino,
Italy

## INTRODUCTION

A properly designed and constructed levee system can often be an effective structural measure for repelling floodwaters and to provide barriers against inundation to protect urbanized and industrial areas. However, the delineation of flood-prone areas and the related hydraulic hazard mapping taking account of uncertainty are usually developed with scarce consideration of the possible occurrence of a levee breach along river channels. The study of critical flood wave routing is typically carried out by assuming that the levee system remains undamaged during the passage of flood because it is designed not to fail. However, flooding is often the result of levee failures and, hence, the vulnerability of levee systems needs to be properly investigated. Different countries worldwide already use levee risk assessment methods developed in the context of research activities addressed to understanding and predicting failure modes (e.g., in the USA, UK, and the Netherlands).

The levee failures can be caused by several factors (ASCE 2011; ICOLD 2013): (1) overtopping, (2) scouring of the foundation, (3) seepage/piping of levee body/foundation, and (4) sliding of the foundation. The piping caused by seepage is one of the most dominant failure mechanisms (Cheng 1993; Colleselli 1997; USACE 1999), influenced by the levee's geometrical configuration,

doi: 10.2166/nh.2017.101

hydraulic conditions, and material properties (e.g., permeability, cohesion, porosity).

The levee failure caused by internal soil erosion occurs when soil particles are carried away by the hydrodynamic forces of the flowing water. The potential failure modes depend on the location of the internal erosion pathway, e.g., through the levee body, the foundation, from the embankment into the foundation, etc. (ICOLD 2013; Zhang *et al.* 2016) and on the specific internal erosion mechanism, e.g., backward erosion piping, internal migration, scour or internal instability (ICODS 2015). Most of the studies treating the issue of piping (Bligh 1910; Lane 1935; Sellmeijer & Koenders 1991, to cite a few) have stated that the parameters which play a role in this mechanism are the hydraulic head, $H$, the seepage line, $L$, and the configuration and material composition of the potential erosion layer. The stability was identified through a coefficient considered for design purposes and which represents the critical piping gradient, $Hc/L$, with $Hc$ the critical head. The information used about the material composition and the configuration of the sand layer characterizes the different methods. If classical empirical approaches are used (Bligh 1910; Lane 1935), a qualitative indication of the material composition is required, while using more advanced approaches (Sellmeijer & Koenders 1991; Nagy & Toth 2005; Van Beek *et al.* 2011; Rice & Polanco 2012; Mazzoleni *et al.* 2014a) information regarding variables, such as permeability, grain distribution, and thickness of soil layer are required. The piping process might also occur for levees that are not in direct interaction with rivers as, e.g., transportation embankments (Polemio & Lollino 2011). Recently, agencies responsible for the maintenance of levees acknowledged the role of animal and rodent burrows in adversely impacting the structural integrity of levees (Orlandini *et al.* 2015). In this context, the importance to understand the hydraulic behavior of levees during a flood is of paramount importance and often it is addressed through numerical simulation models (Zumr & Císlerová 2010), the applicability of which may be limited by scarce knowledge of the levee hydraulic properties of soil. Moreover, a combined research based on experiments and conceptual model has been carried out and relevant results are found in the scientific literature, providing more insight on the influence of the dominant material parameters of the piping process (Sellmeijer *et al.* 2011; Van Beek *et al.* 2011).

In this context, developing operational procedures enabling the most vulnerable levees to be identified, even when the hydraulic parameters characterizing the seepage within the body and foundation are not known or partially known, is fundamental (Take & Bolton 2003; Camici *et al.* 2015).

On this basis, it is of considerable interest to do the following:

- Develop simple and practical procedures for assessing levee vulnerability to seepage, in order to investigate quickly the extended levee systems (Mazzoleni *et al.* 2014a). For this purpose, fragility curves (Vorogushyn *et al.* 2009, 2010) might be used in order to identify the most critical points in the levee system where detailed investigations should be performed and from which potential flood-prone areas can be assessed (Aureli & Mignosa 2004; Di Baldassarre *et al.* 2009).
- Implement and make an operational, structured, and continuously updated levee database, to be used as an integrated tool of a decision support system, where a searchable inventory of information is available as a key resource supporting decisions and actions affecting levee safety. Under this umbrella, likewise Vorogushyn *et al.* (2009), but giving solely evidence to the seepage matter Camici *et al.* (2015), proposed a practical procedure for levee vulnerability to seepage based on a simple vulnerability index, which is assessed according to hydraulic and geometric characteristics of the levee and taking into account uncertainty in the hydraulic parameters.

In this context, the procedure developed by Camici *et al.* (2015) is here extended and used to derive fragility curves from which a refined seepage vulnerability index is identified considering the case of dimensionless levees. It is worth noting that the vulnerability is defined as the condition occurring when the seepage line in the embankment intercepts the landside of the levee during the passage of a flood. The proposed approach brings into play not only geometric characteristics, but also the uncertainty linked to the hydraulic soil parameters of embankment, as permeability and porosity, and other quantities, like flood duration and groundwater capacity, all embedded into a single parameter. Moreover, the method focuses on the seepage through the levee body and aims to identify the probability of occurrence of a critical condition,

necessary but not sufficient, that would allow the soil particles' erosion through the levee embankment and potentially lead to the extreme consequence, that is, the levee piping and the resulting longitudinal structure collapse.

The analysis is of interest for decision-makers to easily estimate the seepage probability of levees of which only the geometry is known. The procedure is embedded in the Italian earthen levee database (*Database nazionale Argi-Nature in TErra, DANTE*) addressed at civil protection purposes. Indeed, DANTE aims to collect comprehensive information on national levees and historical breach failures to be exploited in the framework of operational management and monitoring of levees that form the basis to initialize the seepage vulnerability procedure. Two embanked rivers in Italy are used to show the potential of seepage vulnerability methodology also in the framework of the DANTE database.

## LEEVE VULNERABILITY TO SEEPAGE

The internal erosion of embankments occurs when soil particles are carried away, typically in suspension, by the hydrodynamic forces of the flowing water in the levee body or foundation. Internal erosion potential failure modes can be grouped in different categories related to the physical location of the erosion pathway: through the levee body, through the foundation, from the embankment into the foundation, along the embankment–foundation contact, along or into embedded structures such as conduits or spillway walls (ICOLD 2013; Zhang *et al.* 2016). Moreover, various specific internal erosion mechanisms can occur: backward erosion piping, internal migration (stoping), scour, internal instability (suffusion and suffosion) (for more details see http://www.usbr.gov/ssle/damsafety/risk/BestPractices/Chapters/IV-4-20150617.pdf).

The description of the seepage flows within the levee body is significantly affected by the uncertainty in the soil parameters' estimate, such as the particle size distribution and the soil porosity and hydraulic conductivity (Vorogushyn *et al.* 2009). To overcome this issue, fragility curves taking the soil hydraulic parameters' uncertainty into account would allow the effective estimation of the probability that the seepage line in the levee body intercepts the landside, and as a consequence, to identify the vulnerability to seepage. Under this logical framework, an expeditious procedure, based on a simple vulnerability index, is proposed and described herein.

### Vulnerability index and fragility curves

Let us consider a levee with known geometry by using the quantities $L$ = foot levee, $H$ = saturation depth of infiltration line along the horizontal distance, $x$, and $H_s$ = levee depth (see Figure 1).

To assess the length of the seepage pathway, many solutions of the classical 'heat equation' may be used (Pavlovsky 1960; Marchi 1961; Supino 1965; Ahmad *et al.* 1993; Chahar 2004, to cite a few).

In this study, the solution proposed by Marchi (1961) is applied considering, however, the distinction between embankment and foundation soil:

$$\begin{aligned} H(x) &= h_0\left[1 - erf\left(\frac{x}{2}\sqrt{\frac{\xi}{K_s H_0 D}}\right)\right] \\ &= (h_0' + a)\left[1 - erf\left(\frac{x}{2}\sqrt{\frac{\xi}{K_s H_0 D}}\right)\right] \\ &= h_0'\left[1 - erf\left(\frac{x}{2}\sqrt{\frac{\xi}{K_s H_0 D}}\right)\right] + a\left[1 - erf\left(\frac{x}{2}\sqrt{\frac{\xi}{K_s' H_0 D}}\right)\right] \end{aligned} \quad (1)$$

where $h_0$ = hydraulic head in the river above the water table $= (h_0' + a)$, with $h_0'$ = maximum water level in the main river channel above river bed, $a$ = distance between the groundwater level and the river bed. Moreover, $\xi$ is the soil porosity, $K_s$ and $K'_s$ are the soil hydraulic conductivity of the levee body and foundation, respectively, $H_0$ is the water table below the levee, $D$ is the duration of flood and *erf* represents the error function, i.e., twice the integral of the Gaussian distribution with zero mean and variance equal to 0.5. Focusing on the seepage within the levee body solely, the first term of the right-hand side of Equation (1) is solved to identify the distance at which the seepage line intercepts the ground level ($h = 0$), i.e., the maximum length of the seepage line, $x_{max}$ (Figure 1). If the saturation line is embedded in the embankment, the line does not intercept the levee landside, therefore the seepage is assumed avoided. In this context, Equation (1) is rewritten for a

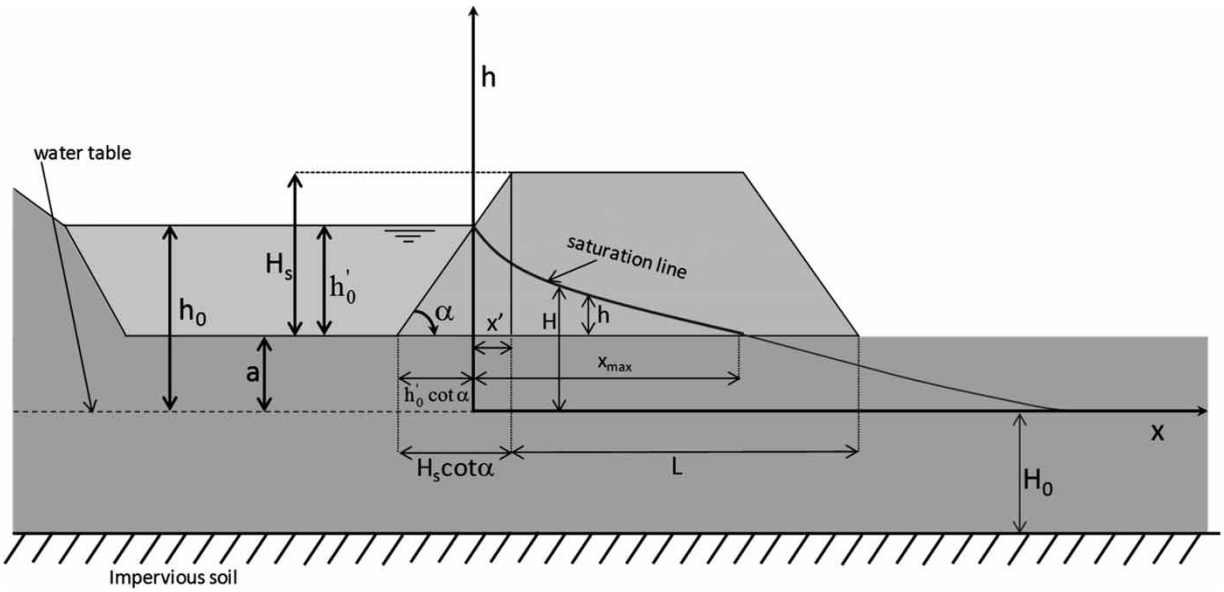


**Figure 1** | Vulnerability index to seepage for a levee with known geometry (for symbols see text).

dimensionless levee and where the parameter $a$ is assumed equal to zero ($H = h$, see Figure 1), yielding:

$$h^*(x^*) = \frac{h_0'}{H_s}\left[1 - erf\left(\frac{x^*}{2\sqrt{K_s\delta}}\right)\right] \quad (2)$$

with $x^* = x/L$ and $h^* = H/H_s$ and the quantity $\delta$ is defined as:

$$\delta = \frac{H_0 D}{L^2 \xi} \quad (3)$$

Equation (2) involves parameters such as $K_s$ and $\delta$ that cannot be easily determined by simple monitoring.

The dimensionless maximum length of the seepage line, $x^*_{\max} = x_{max}/L$, is then identified by imposing $h^* = 0$ in Equation (2). The location of the seepage line is fundamental because it allows identification of the condition, necessary but not sufficient, for which the process may produce erosion up to the extreme consequence, that is the levee piping and the inevitable collapse. If the saturation line is embedded in the embankment, then the piping is surmised avoided, otherwise the seepage condition within the levee body would enable the piping (internal erosion).

In this context, the limit state function, $Z$, for the occurrence of piping is related to the length $(1 + x'^*)$ versus the maximum seepage length $(x^*_{\max})$ along the foot levee itself. Specifically, for the dimensionless levee the simple function is (see Figure 1 for symbols):

$$Z = (1 + x'^*) - x^*_{\max}(t) \quad (4)$$

where $x'^* = (1 - h_0'^*)\cot(\alpha)$, with $\alpha =$ slope of the levee riverside and $h_0'^* = h_0'/H_s$ (see Figure 1).

Based on Equation (4), the levee vulnerability to seepage is finally quantified through a practical vulnerability index, $I_{Vsee}$, defined as:

$$I_{Vsee} = 1 - \frac{(1 + x'^*)}{x^*_{\max}} \quad (5)$$

Specifically, when $I_{Vsee} < 0$, the seepage line is included within the levee body, while when $I_{Vsee} \geq 0$ the seepage line intercepts the levee landside. Based on that, the higher the vulnerability index value the higher the vulnerability to seepage.

Based on Equation (5), the dimensionless and generally applicable fragility curves can be identified using a Monte Carlo sampling method to take the uncertainty on hydraulic levee parameters into account. For instance, Mazzoleni *et al.* (2014b) randomized with a Monte Carlo approach the geometry of the levee to assess fragility curves.

Among the parameters affecting the vulnerability index estimate, $K_s$ and $\xi$ are those typically unknown, whose estimate is characterized by high uncertainty if actual levees are

considered. For that purpose, the sensitivity of the seepage line to the two parameters is first analyzed in this study to identify the most relevant parameter in the process description. Through a Monte Carlo approach and considering the probability distribution of $K_s$ and $\xi$ given in Vorogushyn *et al.* (2009), 1,000 $K_s$ values are randomly sampled from a log-normal distribution with mean $\mu_{Ks} = 10^{-5}$ ms$^{-1}$ and standard deviation $\sigma_{Ks} = 25\mu_{Ks}$ (USACE 1999; Pohl 2000). Assuming $\xi = 0.188$, 1,000 seepage lines given by Equation (1), with $a = 0$, are computed and plotted in Figure 2(a). Likewise, 1,000 seepage lines (see Figure 2(b)) are generated for a fixed value of $K_s = 10^{-5}$ ms$^{-1}$ and a randomly sampled 1,000 different $\xi$ values from a normal distribution with mean $\mu_\xi = 0.188$ and standard deviation $\sigma_\xi = 0.15\mu_\xi$ (Kanowshi 1977; Vorogushyn *et al.* 2009). As can be seen from Figure 2, the seepage line is more sensitive to the hydraulic conductivity, $K_s$, rather than the value of the soil porosity, $\xi$ (USACE 1999; Pohl 2000; Vorogushyn *et al.* 2009).

Considering that the vulnerability is based on the seepage line, Equation (5), depending on $K_s$ and $\delta$, the latter characterizing the dependency of the seepage estimation from the flood duration, the foot levee and the water table, the fragility curves are developed considering the uncertainty in these two parameters through the following procedure:

1. The uncertainty of the hydraulic conductivity value, identified as the most relevant parameter through the sensitivity analysis described above, is addressed by randomly generating 10,000 new $K_s$ values from the log-normal distribution as defined above (Vorogushyn *et al.* 2009). In this case, there may be a wide variability for $K_s$ ($10^{-9}$ and $10^{-3}$ m/s), evidence for which is also given by different works (e.g., USACE 1993; Fenton & Griffiths 1996; Pohl 2000). Moreover, such a wide variability allows taking into account the effect of seepage through both clays ($K_s$ in the range $10^{-8} \div 10^{-12}$ m/s) and soils characterized by higher permeability ($K_s$ up to $10^{-4}$ m/s).
2. The range of variability of $\delta$ is identified on the basis of the maximum and minimum values for $H_0$, $D$, $L$, and $\xi$. Assuming the range of variability of $L$ (3–60 m), $H_0$ (1–50 m), $D$ (12–48 h), and $\xi$ (0.095–0.288; Kanowski 1977), $\delta$ is varied from 80 to $10 \times 10^6$ s/m. Considering a uniform distribution, 10,000 values of $\delta$ are considered, and for each one, 10,000 value of $K_s$ randomly sampled are associated. Therefore, $10^8$ pairs of ($K_s$, $\delta$) are then generated.
3. For all possible pairs ($K_s$, $\delta$), $x^*_{\max}$ is computed through Equation (2) for different $h'_0/H_s$ values, essentially depending on the return period of the flood.
4. The vulnerability index is thus assessed by using Equation (5).

By way of example, the fragility curves are shown in Figure 3(a) and 3(b) for a fixed $h'_0/H_s$ value and for a selected levee for which the geometry is known. Three $\delta$ values (referred to as delta$_1$, delta$_2$, and delta$_3$) are shown between all the plausible values (defined during step 2). They refer to the same triplet ($L$, $H_0$, $\xi$) at which three different durations of the flood wave equal to 12, 24, and 48 hours are associated, thus showing the time-dependency of the fragility curves. Figure 3(a) plots the seepage vulnerability index, $I_{Vsee}$, as a function of $K_s$, while Figure 3(b) provides for each $\delta$ value the cumulative probability of $I_{Vsee}$. From

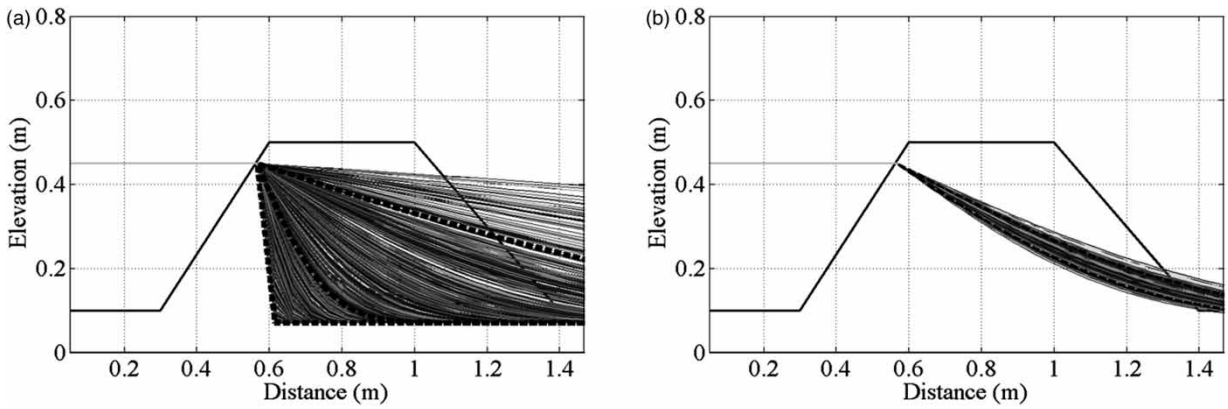


**Figure 2** | Phreatic lines for: (a) different values of the hydraulic conductivity, $K_s$, with $\xi = 0.188$ and (b) different values of the soil porosity, $\xi$, with $K_s = 10^{-5}$ ms$^{-1}$.

an operational point of view, by assigning the geometric characteristics of levee along with the porosity value, it is possible to assess the vulnerability of levee for different durations of flood. For instance, for delta$_2$ ($D = 24$ h), the probability of no-seepage ($I_{Vsee} \leq 0$) is equal to about 0.4, while the complementary 0.6 value represents the probability of seepage occurrence. Moreover, it is worth noting that the cumulative frequency for $I_{Vsee} = 0$ is found equal to 0.3 for delta$_1$, 0.4 for delta$_2$, and higher than 0.5 for delta$_3$. Therefore, as expected, a longer duration corresponds to a higher vulnerability to seepage.

### Seepage vulnerability diagrams

Using the above procedure, for each $I_{Vsee}$ the probability distribution of vulnerability can be expressed as a function of $\delta$ (Camici *et al.* 2015) from which a diagram for an operational vulnerability assessment can be identified for each riverside slope, $\alpha$, and $h'_0/H_s$ value.

A diagram is shown in Figure 4 for two characteristic riverside slope values: 1/2 ($\alpha \cong 27^\circ$) and 2/3 ($\alpha \cong 34^\circ$). In this way, an expeditious assessment of levee vulnerability to seepage, i.e., seepage probability, is made and can be used when the levee geometry, the flood duration, $D$, and the maximum water depth, i.e., the $h'_0/H_s$ ratio, are known. Based on the computed seepage probability, different classes can be identified:

Seepage probability $< 0.3 \rightarrow$ low vulnerability;
$0.3 \leq$ Seepage probability $< 0.6 \rightarrow$ mean vulnerability;
Seepage probability $\geq 0.6 \rightarrow$ high vulnerability.

The limits of the vulnerability classes are identified as a first attempt for levee classification. However, the classes can be modified and adapted to the needs and requirements of the decision-makers by introducing, for instance, a much lower limit (i.e., 0.01) for identifying the levees with very low vulnerability.

Specifically, $\alpha$ value allows the reference diagram for the levee of interest to be selected. Then, $\delta$ and $h'_0/H_s$ are assigned and by selecting the relevant curve it is possible to identify the seepage probability and, hence, the vulnerability class.

## CASE STUDIES

The proposed procedure was applied for a large dataset of levees from different Italian basins. Among them, the case studies of the Tiber River basin, central Italy, and the Tanaro River in the Po River basin, northern Italy, are presented herein.

A reach 152 km long was selected in the Upper Tiber River basin, between the artificial lake of Montedoglio and Monte Molino gauged section subtending a drainage area of 5,279 km$^2$ (see Figure 5(a)). Specifically, levees 33 and 34 are identified on the left and right river side, respectively.

The main channel of the Tanaro River, the major right tributary of the Po River, is 276 km long and the total drainage

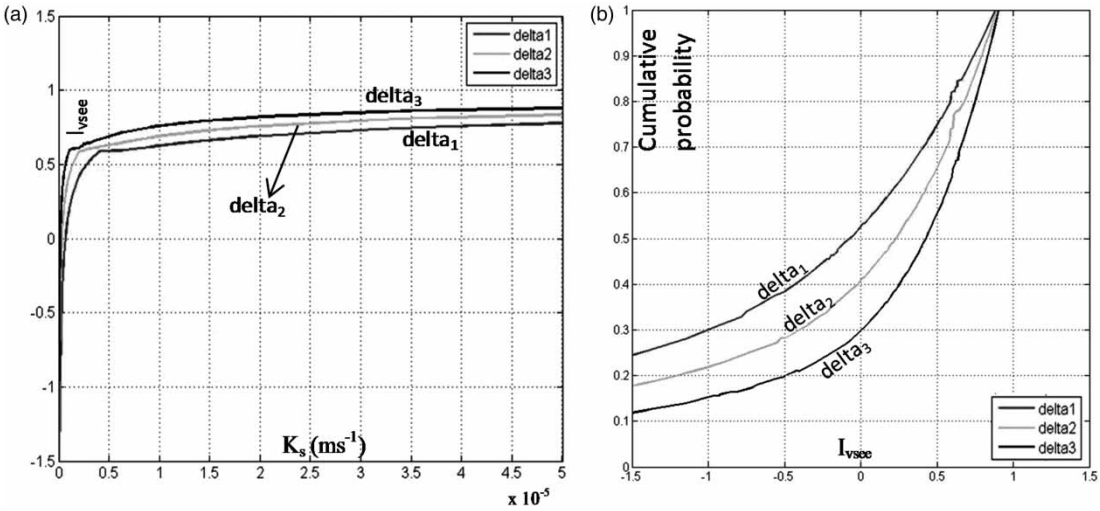


**Figure 3** | Fragility curves for a fixed value of $h'_0/H_s$: (a) $K_s$, $I_{Vsee}$ and (b) $I_{Vsee}$, cumulative probability. $\delta$ (delta) value increases from delta$_1$ to delta$_3$.

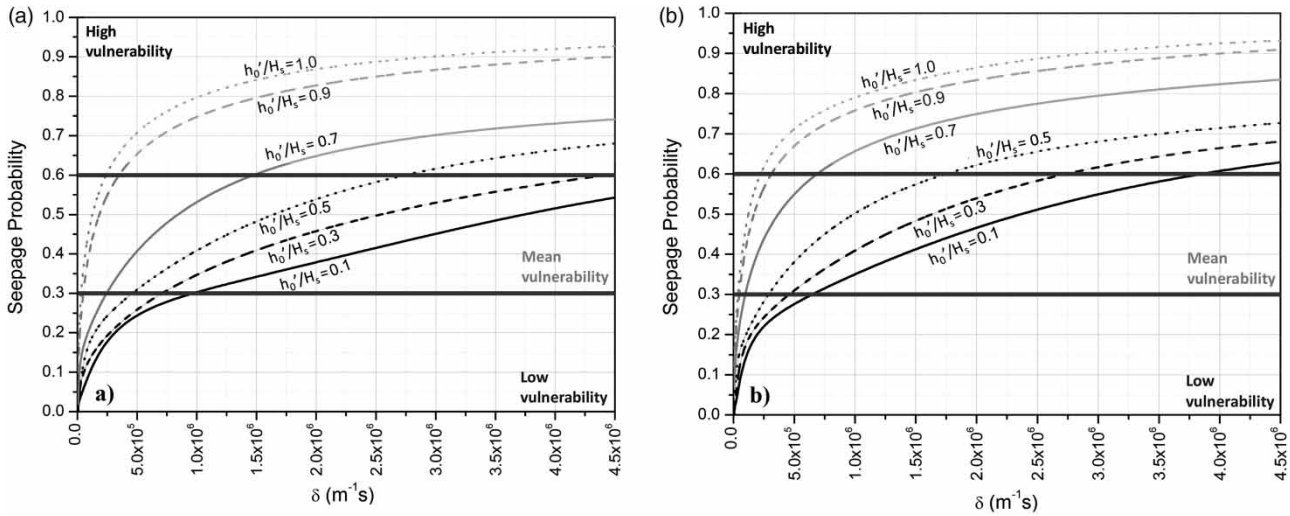


**Figure 4** | Seepage vulnerability diagram for riverside slope equal to: (a) 1/2 ($\alpha \cong 27^{\circ}$) and (b) 2/3 ($\alpha \cong 34^{\circ}$). For symbols see text.

area is about 8,324 km$^2$ (Figure 5(b)). The analysis was focused on the river reaches close to the main urban areas. A total number of six levees were selected, two on the left side near Cherasco city and the remaining levees identified are on both sides of the river, of which two are within Alessandria city, just upstream of the confluence with the Po River.

All available data were collected for the investigated levees and relevant technical-logistic record cards developed, as well as providing geometrical information for levee vulnerability assessment.

## RESULTS

All the levees selected along the Tiber and the Tanaro River were analyzed through the proposed procedure to estimate their vulnerability to seepage.

The results provided by the fragility curves were finally verified through a comparison with levee failures occurring in the past during flood events. The analysis was implemented in the framework of the Italian Levee Database addressed to Civil Protection activities.

### Seepage vulnerability

For the longitudinal structures along the Tiber River, $H_0$ was assumed equal to 15 meters, $\xi$ was set equal to 0.1 and three different relevant flood wave durations, i.e., 12, 24, and 48 hours, were considered. The analysis was carried out for three different return periods (50, 200, and 500 years), each one identifying a value of the $h_0'/H_s$ ratio.

The results are summarized in Table 1 in terms of classes of vulnerability to seepage along with the computed seepage probabilities, for 50 years' return period. As can be seen, the proposed expeditious methodology allows to quickly analyze a large dataset identifying the levees characterized by the larger seepage probabilities, to properly address detailed controls and investigations. In this case, seven levees, shown in italic font in Table 1, are found to be prone to seepage. Overall, for all the flood durations, most of the investigated levees were characterized by a low vulnerability class (specifically, about 45%, 34%, and 25% for $D$ equal to 12, 24, and 48 hours, respectively).

By way of example, the fragility curves developed for the Tv13sx levee are displayed in Figure 6. Tv13sx stands for the '13$^{th}$' levee located on Tiber, Tv, in left river side, sx. As can be seen, this levee is found to be characterized by high vulnerability (seepage probability = 0.68) when the 48 hr flood wave duration was considered.

In Table 1, the river sections where a breach occurred during the flooding event on November 2005 having a magnitude of 50 years and duration of about 30 hours are shown in bold. As can be seen, the procedure estimates mean/high vulnerability for those levees that collapsed during the event without overtopping. Only for the Tv17sx levee, affected by a breach during the flood, the procedure provides a low vulnerability to seepage. In this case, a detailed study should be

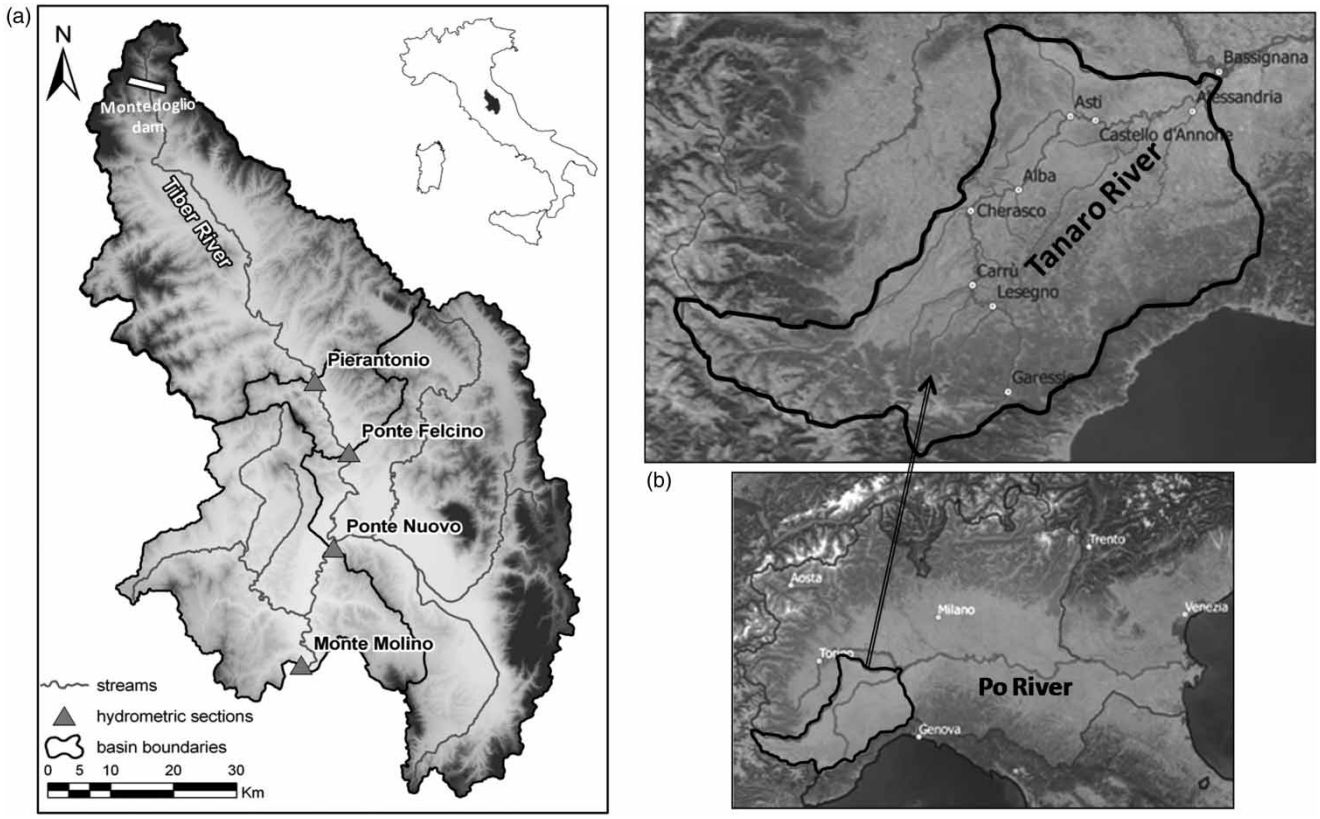


**Figure 5** | Case studies: (a) Tiber River basin, central Italy; (b) Tanaro River basin, northern Italy.

carried out to investigate whether the failure event was due to the external factors as, for instance, the presence of animal/rodent burrows (Camici *et al.* 2015).

For the Tanaro (Ta) River, $H_0$ and $\xi$ are set equal to 30 meters and 0.1, respectively. The same flood durations, i.e., 12, 24, and 48 hours, are considered for the analysis that is carried out only for 200 years' return period. The results, summarized in Table 2, show that two of the investigated levees are overtopped; one is characterized by low vulnerability, while three are found prone to seepage. Specifically, for Ta1sx and Ta2dx the highest probabilities are computed and are found higher than 0.55 when the longest flood duration is considered. Figure 7 shows the results for Ta1sx that is characterized by mean vulnerability for all the investigated flood durations.

It is worth noting that the information on historical levee breaches along the Tanaro River substantially supports the results of the analysis. Specifically, during the very severe flood that affected the Po River basin on November 1994 with a magnitude of nearly 200 years: the Ta2sx and Ta1dx levees collapsed because overtopping occurred; the three most vulnerable levees identified by the proposed methodology, i.e., Ta1sx, Ta2dx, and Ta3dx, were affected by failure processes; for Ta4dx levee, characterized by very low seepage probabilities, there is no evidence of structural failure.

## National levee database

The vulnerability procedure is embedded in a dynamic geospatial database (*Database nazionale delle ArgiNature in TErra, DANTE*), recently developed by CNR-IRPI for the Italian Civil Protection Department of the Presidency of Council of Ministers. DANTE collects data on levee properties and historical levee failures that have been structured in such a way that the presented vulnerability procedure can be used directly by decision-makers. For that, DANTE is structured as a dynamic geospatial tool useful for sharing and managing levee information in one common place and in

**Table 1** | Tiber River: class of vulnerability to seepage (and seepage probability) for the investigated levees for the $h'_0/H_s$ ratio computed for a return period of 50 years ($D$ = flood wave duration)

| | Vulnerability class (seepage probability) | | | | Vulnerability class (seepage probability) | | |
|---|---|---|---|---|---|---|---|
| **Left side levee** | **D = 12 hr** | **D = 24 hr** | **D = 48 hr** | **Right side levee** | **D = 12 hr** | **D = 24 hr** | **D = 48 hr** |
| Tv1sx | overtopping | overtopping | overtopping | *Tv1dx* | *high (0.60)* | *high (0.69)* | *high (0.74)* |
| Tv2sx | overtopping | overtopping | overtopping | Tv2dx | overtopping | overtopping | overtopping |
| Tv3sx | low (0.04) | low (0.06) | low (0.09) | Tv3dx | overtopping | overtopping | overtopping |
| Tv4sx | mean (0.34) | mean (0.41) | mean(0.56) | Tv4dx | low (0.10) | low (0.16) | low (0.22) |
| Tv5sx | mean (0.34) | mean (0.43) | mean (0.58) | Tv5dx | overtopping | overtopping | overtopping |
| Tv6sx | overtopping | overtopping | overtopping | Tv6dx | overtopping | overtopping | overtopping |
| Tv7sx | overtopping | overtopping | overtopping | Tv7dx | low (0.24) | mean (0.33) | mean (0.38) |
| Tv8sx | low (0.03) | low (0.05) | low (0.07) | Tv8dx | low (0.01) | low (0.03) | low (0.05) |
| Tv9sx | low (0.01) | low (0.03) | low (0.04) | **Tv9dx** | overtopping | **overtopping** | **overtopping** |
| Tv10sx | low (0.01) | low (0.03) | low (0.05) | ***Tv10dx*** | *mean (0.52)* | ***high (0.66)*** | ***high (0.73)*** |
| Tv11sx | null | null | null | Tv11dx | overtopping | overtopping | overtopping |
| Tv12sx | mean (0.31) | mean (0.36) | mean (0.50) | Tv12dx | low (0.05) | low (0.09) | low (0.15) |
| ***Tv13sx*** | *mean (0.42)* | ***mean (0.56)*** | ***high (0.68)*** | Tv13dx | low (0.29) | mean (0.35) | mean (0.49) |
| **Tv14sx** | low (0.29) | **mean (0.35)** | **mean (0.49)** | Tv14dx | low (0.25) | mean (0.34) | mean (0.40) |
| Tv15sx | low (0.25) | mean (0.34) | mean (0.40) | Tv15dx | null | null | null |
| Tv16sx | low (0.22) | low (0.29) | mean (0.35) | **Tv16dx** | low (0.29) | **mean (0.35)** | **mean (0.49)** |
| **Tv17sx** | low (0.05) | **low (0.07)** | **low (0.11)** | Tv17dx | low (0.14) | low (0.21) | low (0.26) |
| Tv18sx | low (0.19) | low (0.23) | mean (0.30) | Tv18dx | low (0.11) | low (0.20) | low (0.24) |
| Tv19sx | low (0.22) | low (0.29) | mean (0.35) | Tv19dx | low (0.21) | low (0.25) | mean (0.34) |
| Tv20sx | low (0.14) | low(0.21) | low (0.26) | Tv20dx | low (0.22) | low (0.29) | mean (0.35) |
| Tv21sx | low (0.08) | low (0.14) | low (0.21) | Tv21dx | low (0.21) | low (0.26) | mean (0.34) |
| Tv22sx | null | null | null | Tv22dx | low (0.26) | mean (0.34) | mean (0.42) |
| Tv23sx | overtopping | overtopping | overtopping | Tv23dx | low (0.15) | low (0.22) | low (0.28) |
| Tv24sx | null | null | null | Tv24dx | low (0.12) | low (0.20) | low (0.24) |
| Tv25sx | null | null | null | Tv25dx | null | null | null |
| Tv26sx | null | null | null | Tv26dx | null | null | null |
| Tv27sx | null | null | null | Tv27dx | null | null | null |
| Tv28sx | null | null | null | Tv28dx | null | null | null |
| *Tv29sx* | *mean (0.55)* | *high (0.68)* | *high (0.74)* | Tv29dx | low (0.29) | mean (0.35) | mean (0.49) |
| Tv30sx | null | null | null | *Tv30dx* | *mean (0.49)* | *high (0.64)* | *high (0.72)* |
| Tv31sx | null | null | null | Tv31dx | low (0.08) | low (0.12) | low (0.20) |
| Tv32sx | null | null | null | *Tv32dx* | *mean (0.36)* | *mean (0.49)* | *high (0.63)* |
| Tv33sx | low (0.06) | low (0.09) | low (0.15) | Tv33dx | low (0.10) | low (0.20) | low (0.23) |
| | | | | *Tv34dx* | *mean (0.41)* | *mean (0.56)* | *high (0.67)* |

The levees affected by failure during the severe flood of November 2005 are in bold font.

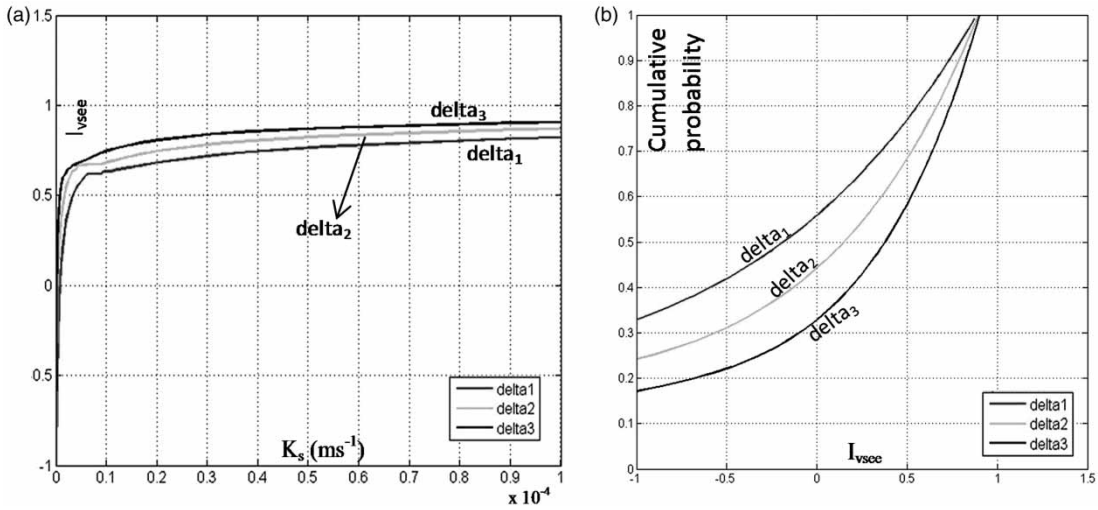


**Figure 6** | Tiber River: fragility curves for the levee Tv13sx for return period = 50 years ($h'_0/H_s = 0.95$) (a) ($K_s$, $I_{Vsee}$) and (b) ($I_{Vsee}$, cumulative probability). Delta$_1$, delta$_2$, and delta$_3$ correspond to flood duration equal to 12, 24, and 48 hours, respectively.

one common structure for national and general public use, supporting authorities with the charge of hydraulic risk mitigation in identifying operationally levee seepage vulnerability. Specifically, DANTE is directed at collecting comprehensive available data about Italian levees and historical breach failures and provide information about: (1)

**Table 2** | As for Table 1, but for the Tanaro River and for a return period of 200 years

| | Vulnerability class (seepage probability) | | | | Vulnerability class (seepage probability) | | |
|---|---|---|---|---|---|---|---|
| **Left side levee** | **D = 12 hr** | **D = 24 hr** | **D = 48 hr** | **Right side levee** | **D = 12 hr** | **D = 24 hr** | **D = 48 hr** |
| ***Ta1sx*** | *mean (0.34)* | *mean (0.42)* | ***mean (0.56)*** | **Ta1dx** | overtopping | overtopping | **overtopping** |
| **Ta2sx** | overtopping | overtopping | **overtopping** | ***Ta2dx*** | *mean (0.34)* | *mean (0.41)* | ***mean (0.57)*** |
| | | | | **Ta3dx** | low (0.28) | mean (0.35) | **mean (0.48)** |
| | | | | Ta4dx | low (0.06) | low (0.09) | low (0.17) |

The levees affected by failure during the severe flood of November 1994 are in bold.

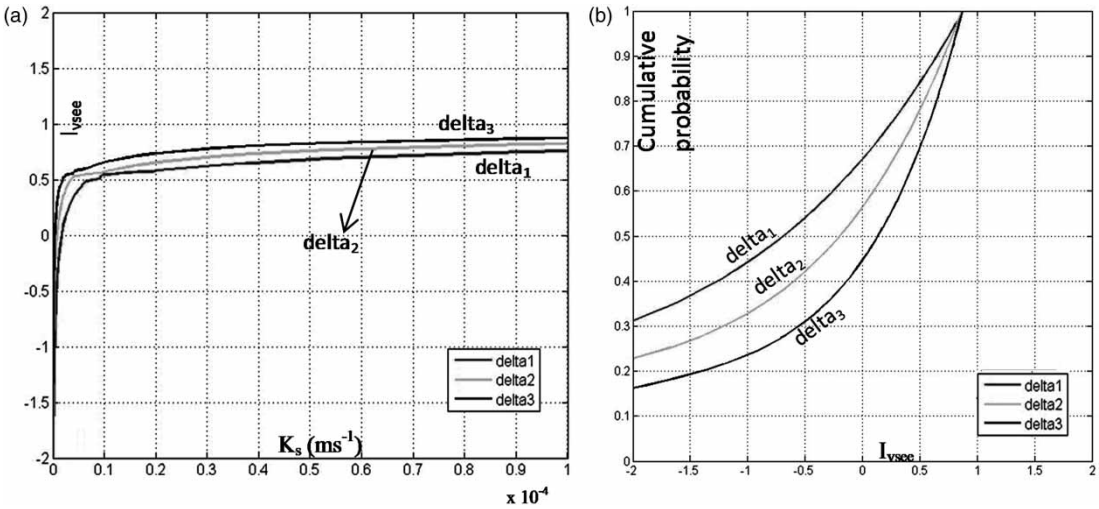


**Figure 7** | As for Figure 6, but for the Tanaro River levee Ta1sx, return period = 200 years ($h'_0/H_s = 0.79$).

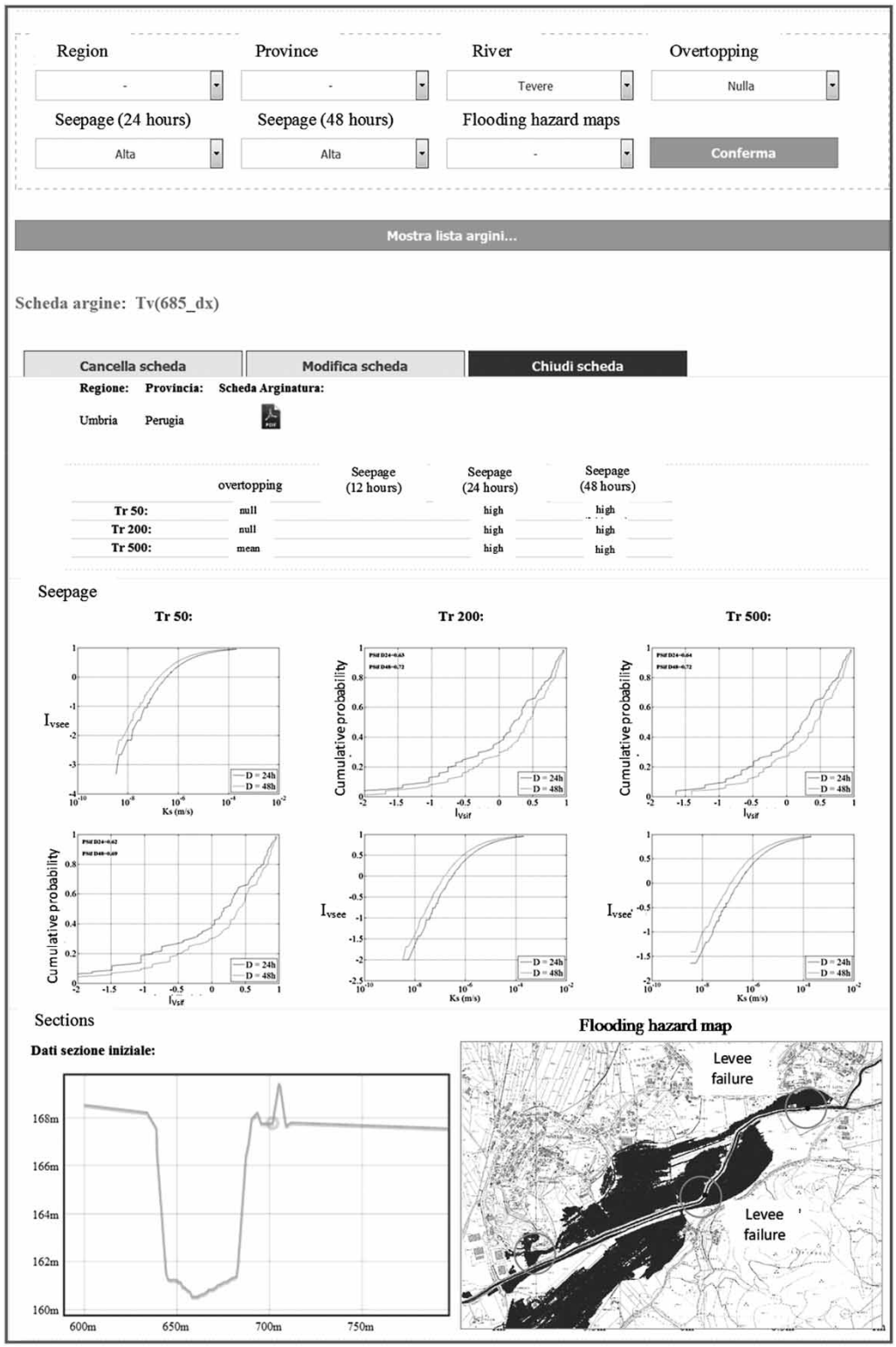


**Figure 8** | DANTE web-page.

location and condition of levees; (2) geometrical properties; (3) photographic documentation; and (4) historical failures. DANTE can be updated in order to include all available and potentially useful information, such as data on the levee material when available.

The vulnerability assessment methodology was implemented for the database so that the assessment of vulnerability to overtopping (Camici *et al.* 2015) and seepage could be addressed. Moreover, information on management, control and maintenance and flood hazard maps developed by assuming the levee system undamaged/damaged during the flood event are provided as well. The database consulting starts from the home page where a set of items (Region, Province, River, etc.) allows the user to select only the levees of interest. As DANTE is mainly directed at public authorities in charge of hydraulic risk prevention and management, the levees' selection can also be based on the vulnerability class to overtopping and/or seepage as well as on the availability of flooding hazard maps. For each levee, the relevant data can be displayed, including a technical-logistic record card, the vulnerability classes to overtopping and seepage and flooding hazard maps with and without levee collapse. Figure 8 shows the main structure of the database along with an example for levees with high seepage vulnerability and flooding map for the Tiber basin. As can be seen, DANTE represents a sound tool since decision-makers can address expeditious assessment of levee embankment vulnerability to seepage and infer the consequent flood-prone areas.

## CONCLUSIONS

A practical and expeditious procedure to evaluate the vulnerability to seepage for earthen levees was enhanced herein and tested for two selected case studies in Italy. At the present, the proposed method is developed considering the seepage line analysis in the embankment only, while future investigations are planned to embed the foundation soil as well. A simple vulnerability index was identified and can be conveniently adopted for levees wherein the hydraulic parameters of soils are unknown or partly known. The procedure takes the uncertainty of the hydraulic parameter into account to estimate the fragility curves and provides the probability of vulnerability of a levee to seepage which quickly enable investigation of the extended levee systems to identify the most likely critical points where detailed investigations are required.

The fragility curves developed herein are a new perspective which enables the estimation of the seepage probability as a function of the water depth in the channel and the quantity $\delta$ depending on the flood duration, the foot levee, the soil porosity, and the water table. Based on these curves, the vulnerability can be easily identified without needing to know the hydraulic conductivity in the embankment, which is a critical parameter not easy to assess.

The results obtained for the Tiber River, in central Italy, and the Tanaro River, in northern Italy, by analyzing 67 and six levees, respectively, compared with the information on historical levee failures suggest that the method seems to be able to identify the most vulnerable levees, for which detailed investigations should be carried out.

The results of the vulnerability analysis are included, along with all the other available data in the Italian levee database (*Database nazionale delle ArgiNature in TErra, DANTE*) recently developed by IRPI-CNR for the Civil Protection Department. DANTE is presented as a dynamic geospatial tool addressed to collect all the available data/information on levee systems and to usefully support authorities with the responsibility of hydraulic risk mitigation.

## ACKNOWLEDGEMENTS

This work was partly supported by the agreement between the Civil Protection Department and the National Research Council-IRPI. We thank the Editor, the anonymous reviewer, Roberto Ranzi and Stefano Barontini for their valuable comments and suggestions.

## REFERENCES

Ahmad, S., Kashyap, D. & Mathur, B. S. 1993 Mathematical modelling of saturated-unsaturated flow to drains. *Journal of Irrigation and Drainage Engineering* **119** (1), 18–33.

ASCE/EWRI Task Committee on Dam/Levee Breaching 2011 Earthen embankment breaching. *Journal of Hydraulic Engineering* **137** (12), 1549–1564.

Aureli, F. & Mignosa, P. 2004 Flooding scenarios due to levee breaking in the Po river. *Proceedings of the Institution of Civil Engineers – Water Management* **157** (1), 3–12.

Bligh, W. G. 1910 Dams, barrages and weirs on porous foundations. *Engineering News Record* **64** (20), 708–710.

Camici, S., Barbetta, S. & Moramarco, T. 2015 Levee body vulnerability to seepage: the case study of the levee failure along the Foenna stream on 1 January 2006 (central Italy). *Journal of Flood Risk Management*. doi: 10.1111/jfr3.12137.

Chahar, B. R. 2004 Determination of length of a horizontal drain in homogeneous earth dams. *Journal of Irrigation and Drainage Engineering* **130** (6), 530–536.

Cheng, S. T. 1993 Statistics of dam failures. In: *Reliability and Uncertainty Analyses in Hydraulic Design* (B. C. Yen & Y. K. Tung, eds). ASCE, Reston, VA, pp. 97–105.

Colleselli, F. 1997 *Problemi idraulici e strutturali delle arginature in terra (Hydraulic and Structural Issue for Earthen Levees)*, La difesa idraulica del territorio, Ed. Bios, Italy, pp. 107–128.

Di Baldassarre, G., Castellarin, A., Montanari, A. & Brath, A. 2009 Probability weighted hazard maps for comparing different flood risk management strategies: a case study. *Natural Hazards* **50**, 479–496. doi: 10.1007/s11069-009-9355-6.

Fenton, G. A. & Griffiths, D. V. 1996 Statistics of free surface flow through stochastic earth dam. *Journal of Geotechnical Engineering* **122** (6), 427–436.

ICODS (Interagency Committee on Dam Safety) 2015 *Evaluation and Monitoring of Seepage and Internal Erosion*, Federal Emergency Management Agency, FEMA P-1032.

ICOLD 2013 *Internal Erosion of Existing Dams, Levees, and Dikes, and Their Foundations*. Bulletin 164 Preprint, International Commission on Large Dams, Paris, France.

Kanowski, H. 1977 Ein Beitrag zur zerstörungsfreien Untersuchung von Flussdeichen. PhD Thesis, Dresden University of Technology, Germany.

Lane, E. W. 1935 Security from underseepage. *Transactions of the American Society of Civil Engineers* **100**, 1235–1351.

Marchi, E. 1961 Sulla filtrazione attraverso gli argini fluviali (On the infiltration process within levees). In: *Proceedings of VII Convegno di Idraulica e Costruzioni Idrauliche*, Palermo, Italy.

Mazzoleni, M., Bacchi, B., Barontini, S., Di Baldassarre, G., Pilotti, M. & Ranzi, R. 2014a Flooding hazard mapping in floodplain areas affected by piping breaches in the Po River, Italy. *Journal of Hydrologic Engineering* **19** (4), 717–731.

Mazzoleni, M., Barontini, S., Ranzi, R. & Brandimarte, L. 2014b Innovative probabilistic methodology for evaluating the reliability of discrete levee reaches owing to piping. *Journal of Hydrologic Engineering* **20** (5), 04014067.

Nagy, L. & Toth, S. 2005 *Detailed Technical Report on the Collation and Analysis of Dike Breach Data with Regards to Formation Process and Location Factors. Technical Report*, H-EURAqua Ltd., Hungary.

Orlandini, S., Moretti, G. & Albertson, J. D. 2015 Evidence of an emerging levee failure mechanism causing disastrous floods in Italy. *Water Resources Research* **51** (10), 7995–8011. doi: 10.1002/2015WR017426.

Pavlovsky, N. N. 1960 *Collected Works*, Akad, Nauk USSR, Leningrad.

Pohl, R. 2000 Aspekte der Sicherheit von Deichen mit inhomogenem Aufbau. *Wasser Abfall* **11**, 52–57.

Polemio, M. & Lollino, P. 2011 Failure of infrastructure embankments induced by flooding and seepage: a neglected source of hazard. *Natural Hazards and Earth Systems Sciences* **11**, 3383–3396.

Rice, J. D. & Polanco, L. 2012 Reliability-based under seepage analysis in levees using a response surface – Monte Carlo simulation method. *Journal of Geotechical and Geoenvironmental Engineering* **138** (7), 821–830.

Sellmeijer, J. B. & Koenders, M. A. 1991 A mathematical model for piping. *Applied Mathematical Modeling* **115** (6), 646–651.

Sellmeijer, J. B., Lopez De La Cruz, J., van Beek, V. M. & Knoeff, J. G. 2011 Fine tuning of the backward erosion piping model through small scale, medium scale and IJKdijk experiments. *European Journal of Environmental and Civil Engineering* **15** (8), 1139–1154.

Supino, G. 1965 *La filtrazione attraverso gli argini e nelle falde sotterranee (The Filtration Process through Levees and Groundwater)*. Le reti idrauliche. Patron Ed. Bologna, Italy, pp. 439–485.

Take, W. A. & Bolton, M. D. 2003 Tensiometer saturation and the reliable measurement of soil suction. *Géotechnique* **53** (2), 159–172.

USACE 1993 Seepage analysis and control for dams, Engineer Manual.

USACE 1999 Risk-based analysis in geotechnical engineering for support of planning studies. *Engineer Technical Letter*, 1110-2-556, US Army Corps of Engineers.

Van Beek, V. M., Knoeff, J. G. & Sellmeijer, J. B. 2011 Observations on the process of piping by underseepage in cohesionless soils in small, medium and large-scale experiments. *European Journal of Environmental and Civil Engineering* **15** (8), 1115–1137.

Vorogushyn, S., Merz, B. & Apel, H. 2009 Development of dike fragility curves for piping and micro-instability breach mechanisms. *Natural Hazards and Earth System Sciences* **9**, 1382–1401.

Vorogushyn, S., Merz, B., Lindenschmidt, K. E. & Apel, H. 2010 A new methodology for flood hazard assessment considering dike breaches. *Water Resources Research* **46** (8), W08541.

Zhang, L., Peng, M., Chang, D. & Xu, Y. 2016 Dam failure risk assessment. In: *Dam Failure Mechanisms and Risk Assessment*, Chapter 12. John Wiley & Sons Singapore Pte. Ltd, pp. 307–321, http://dx.doi.org/10.1002/9781118558522.ch12.

Zumr, D. & Císlerová, M. 2010 Soil moisture dynamics in levees during flood events – variably saturated approach. *Journal of Hydrology and Hydromechanics* **58** (1), 64–72.

First received 31 March 2016; accepted in revised form 23 November 2016. Available online 8 February 2017